Research Article | Vol. 31, No. 5 / 27 Feb 2023 / Optics Express 7200

Optics EXPRESS

Cavity-enhanced and temporally multiplexed atom-photon entanglement interface

HAILONG LIU,[1,2] MINJIE WANG,[1,2] HAOLE JIAO,[1,2] JIAJIN LU,[1,2] WENXIN FAN,[1,2] SHUJING LI,[1,2,3] AND HAI WANG[1,2,4]

[1]*State Key Laboratory of Quantum Optics and Quantum Optics Devices, Institute of Opto-Electronics, Shanxi University, Taiyuan 030006, China*
[2]*Collaborative Innovation Center of Extreme Optics, Shanxi University, Taiyuan 030006, China*
[3]*lishujing@sxu.du.cn*
[4]*wanghai@sxu.edu.cn*

Abstract: Practical realization of quantum repeaters requires quantum memories with high retrieval efficiency, multi-mode storage capacities, and long lifetimes. Here, we report a high-retrieval-efficiency and temporally multiplexed atom-photon entanglement source. A train of 12 write pulses in time is applied to a cold atomic ensemble along different directions, which generates temporally multiplexed pairs of Stokes photons and spin waves via Duan-Lukin-Cirac-Zoller processes. The two arms of a polarization interferometer are used to encode photonic qubits of 12 Stokes temporal modes. The multiplexed spin-wave qubits, each of which is entangled with one Stokes qubit, are stored in a "clock" coherence. A ring cavity that resonates simultaneously with the two arms of the interferometer is used to enhance retrieval from the spin-wave qubits, with the intrinsic retrieval efficiency reaching 70.4%. The multiplexed source gives rise to a ∼12.1-fold increase in atom-photon entanglement-generation probability compared to the single-mode source. The measured Bell parameter for the multiplexed atom-photon entanglement is 2.21(2), along with a memory lifetime of up to ∼125 μs.

1. Introduction

Realization of entanglement distribution over long distances is a core task for long-distance quantum communications [1,2] and large-scale quantum networks [3]. Direct entanglement distribution over a distance of 1000 km is difficult because of the transmission losses in the fiber channel. Quantum repeaters (QRs) represent a promising solution to overcome this loss problem [1,2]. A QR [4] includes a number of elementary links, each of which is composed of two nodes. An atom-photon entanglement source, i.e., a quantum interface (QI) that generates the entanglement between the photonic and spin-wave (atomic memory) qubits, can be used as a repeater node [5,6]. In each link, quantum memories are deposited at the nodes and the photons are sent to a central station for entanglement generation between two nodes. The quantum memories are then converted into photons for entanglement connections between adjacent links [1,2].

Various mechanisms for optical quantum memories based on atomic ensembles have been studied widely, including electromagnetically-induced transparency (EIT) [7–19], the gradient echo memory (GEM) [20–23], the atomic frequency comb (AFC) [20–34], Raman memory [35–39], and the Duan-Lukin-Cirac-Zoller (DLCZ) protocol [1,40–64] etc. Among these protocols, EIT, GEM, and the AFC are called "read-write" [65] (or "absorptive" [66]) memory schemes, whereas the DLCZ is called a "read-only" memory scheme [65]. Realization of QRs in practice requires quantum memories with high performance characteristics, including high retrieval efficiency, multi-mode storage capacity, and long lifetimes [67,68].

High-efficiency "absorptive" optical memories have been realized using high-optical-depth atomic ensembles [14,16–18,21,39] or by coupling atomic ensembles with a low-finesse optical

#483444 https://doi.org/10.1364/OE.483444
Journal © 2023 Received 13 Dec 2022; revised 19 Jan 2023; accepted 25 Jan 2023; published 13 Feb 2023

Optics EXPRESS

cavity [19,22,69,70]. Use of the EIT scheme in a high-optical-depth cold atomic ensemble allowed the retrieval efficiencies for single photons and single-photon-level qubits to reach 85% [18] and 68% [17], respectively. The retrieval efficiency of optical storage based on the AFC scheme has been improved by using cavity-enhanced atom-photon coupling [22,69]. Efficient DLCZ quantum memories have been realized using low-finesse optical cavities [49–52,60], with retrieval efficiencies of up to ~75% being achieved in these experiments. Long-life memories have been achieved by loading atoms into an optical lattice and using magnetically-insensitive spin waves to store the photons [48, 52,61]. To date, the longest memory lifetime for a qubit memory has reached the order of seconds based on use of an atomic ensemble [60]. When compared with single-mode memories, multiplexed quantum memories represent a promising way to achieve increased entanglement generation rates in each elementary link [25,71–74]. Specifically, if the QRs use QIs that are capable of storing N modes as nodes, the repeater rate will then be increased by a factor of N when compared with those that use single-mode QIs as nodes. In recent years, temporally [53,54,75–81], spatially [55,74,82–84], and spectrally [25,31,85] multiplexed memories for single photons, weak coherent light pulses, or optical quantum states have been demonstrated successfully using solid-state and gaseous-state ensembles of atoms.

Using multiple spatial-channel collections, multiplexed QIs that generate entanglement between a spin-wave qubit and a photonic qubit in six modes have been demonstrated based on a cold atomic ensemble [74]. On the basis of that work [74], a long-lived and spatially-multiplexed atom-photon entanglement interface has been demonstrated [61]. Pu et al. realized a multiplexed DLCZ-type quantum memory with 225 individually accessible memory cells using a macroscopic cold atomic ensemble [55]. Recently, massively-multiplexed DLCZ-type quantum memories have been demonstrated in cold atoms via spatially-resolved single-photon detection [86]. Spin-wave-photon quantum correlations in more than ten temporal modes have been demonstrated using rare-earth ion-doped crystals (solid-state atomic ensembles) via the DLCZ approach [53,75,87]. By applying a train of write pulses to a cold atomic ensemble, with each pulse being sent along different directions, our group previously demonstrated a 19-temporal-mode atom-photon entanglement [81]. A temporally-multiplexed DLCZ-type quantum memory was also realized by applying a reversible gradient magnetic field to a cold atomic ensemble to control the rephasing of the spin waves [88] by Riedmatten's group. Furthermore, their group demonstrated suppression of additional noise generated in the temporal multimode memory using a low-finesse optical cavity [89]. Because the cavity resonates with the "write-out" photons but not with the "read-out" photons, the retrieval efficiency achieved in that experiment has not been enhanced. Recently, Cox et al. experimentally demonstrated coupling of a single optical cavity mode with multiplexed spin waves created by multiple Raman dressing beams at different times and then observed the interference of two spin waves [90].

To date, high-efficiency and multiplexed quantum memories have been demonstrated in separate experiments. For example, in cavity-enhanced atom-photon entanglement sources [51,91], the intrinsic retrieval efficiency has reached ~76%, but the memories used for the photonic qubits are not multiplexed. In the spatially multiplexed DLCZ-type quantum memory used for single photons [92], the number of stored modes is more than 600, and the intrinsic retrieval efficiency is ~35%. In the experiments on temporally-multiplexed DLCZ-type quantum memories, the numbers of stored modes are greater than ten, and the intrinsic retrieval efficiencies are ~4% for the devices using rare-earth ion-doped crystals [53,54] and ~16% in cold atoms [64,81]. To date, there have been no experimental reports of an atom-photon entanglement source having a multiplexed storage capacity and high retrieval efficiency simultaneously.

In the experiment presented here, we demonstrate a cavity-enhanced and temporally-multiplexed atom-photon entanglement interface by combining temporally-multiplexed storage [61] and cavity-enhanced retrieval schemes [91] into a system. A train of 12 write pulses in time is applied to a cold atomic ensemble along different directions, and each of these pulses generates

Optics EXPRESS

a correlated pair of a Stokes photon and an atomic collective excitation (a spin wave) with a small probability based on a DLCZ memory scheme [1]. The cold atomic ensemble is placed at the center of a polarization interferometer. The Stokes fields that are created in a write pulse and emitted into the two arms of the interferometer are then encoded onto photonic qubits. The relative phase between the two arms is stabilized passively. Two spin-wave modes, each of which corresponds to one of the Stokes qubit fields, are used for the spin-wave qubit. All the spin-wave qubits are stored in a "clock" coherence. The photonic and spin-wave qubits created by each write pulse are entangled. The multiplexed spin-wave qubits are mapped into an anti-Stokes photon by applying read beams that are controlled using a feedforward system. A ring cavity that resonates simultaneously with the write-out (Stokes) and anti-Stokes fields propagating along the two arms of the interferometer is used to enhance retrieval of the multiplexed spin waves. The cavity in combination with the interferometer forms a polarization-interferometer-based cavity that was used in our previous experiment [91] to generate a high-retrieval-efficiency (77%) nonmultiplexed atom-photon entanglement. In the experiment presented here, the intrinsic retrieval efficiency of the multiplexed atom-photon entanglement interface reaches $70.4 \pm 1.9\%$. We demonstrate a ~12.1-fold (11.6-fold) probability increase in the generation of entangled atom-photon (photon-photon) pairs when compared with a nonmultiplexed entanglement source. The measured Bell parameter for the multiplexed atom-photon entanglement is 2.21(2), and is combined with a memory lifetime of up to ~125 μs.

2. Experimental setup

Figure 1(a) shows a schematic diagram of our experimental setup, in which a cold ^{87}Rb atomic ensemble with an optical density of 16 is used as the memory medium. To generate pairs composed of a Stokes photon and a spin wave in temporally multiplexed modes, we apply a train of write pulses, each of which is incident along a different direction onto the atoms. A scheme of this type was demonstrated in our previous publication [81]. The main improvement in this work is that a ring cavity is applied to improve the retrieval efficiency. As shown in Fig. 1(a), the ring cavity is formed using three high-reflection mirrors ($HR_{1,2,3}$) and an output coupler (OC) with reflectance of 80%. The cavity supports the TEM_{00} mode, which is labeled as A_{00} in Fig. 1(a). To encode the Stokes photons onto qubits, we inserted a polarization interferometer that is formed using beam displacers BD_1 and BD_2 in the cavity. This polarization-interferometer-based cavity is the same as that used in our previous experiment [91], where cavity-enhanced single-mode atom-photon entanglement was demonstrated. When the interferometer is inserted into the cavity, an arbitrarily-polarized field propagating in the A_{00} mode along the clockwise (counterclockwise) direction will be split into H (horizontally) and V (vertically) polarized components by BD_2 (BD_1). The H-polarized (V-polarized) field is directed into arm A_L (A_R) of the interferometer. Two optical lenses, L_1 and L_2, are inserted in the interferometer and make the arms A_L and A_R pass crossways through the atomic ensemble. More details on our polarization-interferometer-based cavity can be found in the report on our previous experiment in the literature [91].

The relevant energy levels are shown in Fig. 1(b). To define the quantization axis, we apply a bias magnetic field ($B_0 = 4\,G$) to the atomic ensemble. The ground states $|g\rangle = |5S_{1/2}, F = 1\rangle$ and $|s\rangle = |5S_{1/2}, F = 2\rangle$ combine with one of the excited states $|e_1\rangle = |5P_{1/2}, F' = 1\rangle$ or $|e_2\rangle = |5P_{1/2}, F' = 2\rangle$ to form a Λ-type atomic system. The atoms are initially prepared into the state $|g, m_F = 0\rangle$ via optical pumping. The atom-photon entanglement generation process then follows. At the beginning of a trial, a train of m (ranging up to 12) write pulses is applied to the atoms through beam splitter BS_1 [Fig. 1(a)]. The m write pulses are applied around z-axis and along m different directions, corresponding to m wave-vectors $\mathbf{k}_w^j$ with $j = 1$ to m. The write pulses are then σ^+-polarized and red-detuned from the $|g\rangle \rightarrow |e_1\rangle$ transition by 110 MHz. Each of these write pulses induces the Raman transition $|g, m_{F_g} = 0\rangle \rightarrow |s, m_{F_s} = 0\rangle$ via $|e_1, m_{F_{e1}} = 1\rangle$ [see Fig. 1(b)], which emits σ^+-polarized Stokes photons and simultaneously creates spin-wave

Optics EXPRESS

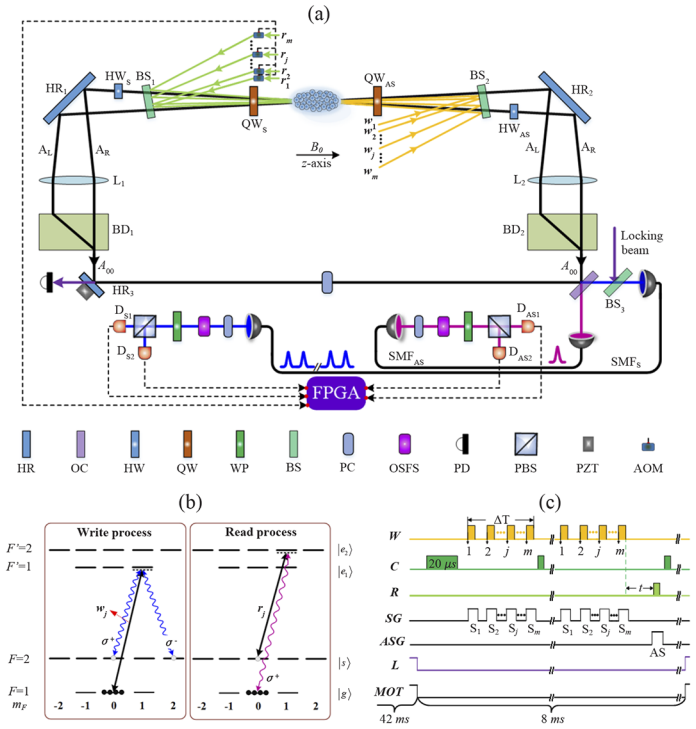

Fig. 1. Overview of the experiment. (a) Experimental setup. HR_1, HR_2, HR_3: high-reflectivity mirrors; OC: output coupler; HW (QW): half-wave (quarter-wave) plate; WP: wave plate; BS_1, BS_2, BS_3: beam splitters; PC: phase compensator; OSFS: optical-spectrum-filter set; PD: photodiode; PBS: polarizing beam splitter; PZT: piezoelectric transducer; AOM: acoustic optical modulator; L_1, L_2: lenses; BD_1, BD_2: beam displacers; SMF_S, SMF_{AS}: single-mode fibers; D_{S1}, D_{S2}, D_{AS1}, D_{AS2}: single-photon detectors; FPGA: field programmable gate array; w_1, w_2, $\cdots$ w_j $\cdots$ w_m: write pulses ($\theta_{w_l,w_k} \geq 0.20^\circ$ ($l,k \in m$ and $l \neq k$)); r_1, r_2, $\cdots$ r_j $\cdots$ r_m: read pulses; B_0: bias magnetic field. The free spectral range of the cavity is approximately 66.7 MHz and the finesse is measured to be ~16. The angle between A_L and A_R is $\theta_{A_L,A_R} \approx 0.21^\circ$. Both Stokes and anti-Stokes photon qubits are required to resonate with the ring cavity. To meet this requirement, an H-polarized cavity-locking beam is injected from the OC into the cavity to stabilize the cavity length using a Pound-Drever-Hall locking scheme. The H-polarized Stokes and anti-Stokes photons are made to resonate with the cavity by varying the position of cavity mirror HR_3, which is attached to a manual translation stage. The V-polarized photons are adjusted to resonate by adjusting the WPs of the PC. (b) Relevant atomic levels. (c) Time sequence for the experimental trials. W, C, R: write, cleaning, and read laser pulses. SG (ASG): Timeline of the S (AS) detector gate; the sizes of the detection windows denoted by S_1, S_2 $\cdots$ S_j $\cdots$ S_m and AS are all ~250 ns; L: locking beam gate; MOT: magneto-optical trap gate. The experimental period is 50 ms, of which 42 ms is used for cold atom preparation, and the remaining 8 ms is used for atom-photon entanglement generation. We stabilize the cavity length intermittently during the cold atom preparation phase. A two-dimensional MOT of 41.5 ms and a subsequent Sisyphus cooling stage of 0.5 ms cool the atomic cloud to 100 μK. A train of 12 write pulses lasts for $\Delta T = 8$ μs. If a Stokes photon is detected in the window of S_j, then the corresponding jth reading light pulse is switched on after a storage time t to convert the spin wave into an anti-Stokes photon via the feedforward-controlled readout system, which mainly consists of an FPGA and an AOM. After the retrieval process, a cleaning pulse is applied to empty the atomic memory. If no Stokes photons are detected in any of the detection windows, the cleaning pulse is then applied directly to start the next write-read-clean trial period.

Optics EXPRESS

(SW) excitations associated with the "clock" coherence $|m_{F_g}=0\rangle \leftrightarrow |m_{F_s}=0\rangle$. During the interaction of the atoms with the jth write pulse, if a Stokes photon is emitted into the cavity mode A_R (A_L) and propagates along the counterclockwise direction, it is then called S_R^j (S_L^j). Along with emission of the photon S_R^j (S_L^j), an atomic excitation in the SW mode M_R^j (M_L^j) defined by the wave-vector $\mathbf{k}_{M_R}^j = \mathbf{k}_w^j - \mathbf{k}_{S_R}$ ($\mathbf{k}_{M_L}^j = \mathbf{k}_w^j - \mathbf{k}_{S_L}$) will be created, where $\mathbf{k}_{S_R}$ ($\mathbf{k}_{S_L}$) denotes the wave-vector of the Stokes photons S_R^j (S_L^j) with $j=1$ to m. The σ^+-polarized Stokes photons S_R^j and S_L^j are transformed into H-polarized fields by a $\lambda/4$-wave plate labeled as $\mathrm{QW_S}$ in Fig. 1(a). Furthermore, the H-polarized S_R^j is transformed into a V-polarized field by a $\lambda/2$-wave-plate that is labeled as $\mathrm{HW_S}$ in Fig. 1(a). These fields are combined into the cavity mode A_{00} by $\mathrm{BD_1}$ and then form a Stokes qubit S_{qbit}^j. As shown in Fig. 1(b), the write pulse also induces the Raman transition $|g, m_{F_g}=0\rangle \rightarrow |s, m_{F_s}=2\rangle$ via $|e_1, m_{F_{e1}}=1\rangle$, which emits σ^--polarized Stokes photons. When a σ^--polarized Stokes photon is directed into the A_R (A_L) mode along the counterclockwise direction, it will be transformed into an H- (V-) polarized photon by the $\lambda/4$-wave-plate $\mathrm{QW_S}$ ($\mathrm{QW_S}$ together with $\mathrm{HW_S}$) and is then excluded from the A_{00} cavity mode by $\mathrm{BD_1}$.

The atom-photon joint state created by the jth write pulse can be written as $\rho^j = |0\rangle^{jj}\langle 0| + \chi_j |\Phi\rangle_{ap}^j{}_{ap}^j\langle\Phi|$, where $|0\rangle^j = |0\rangle_{S_j}|0\rangle_{M_j}$ denotes the vacuum state, $\chi_j \ll 1$ is the excitation probability induced by the jth write pulse, and $|\Phi\rangle_{ap}^j$ is the entanglement state between the spin-wave qubit encoded onto the M_R^j and M_L^j modes and the Stokes qubit S_{qbit}^j. This state is written as:

$$|\Phi\rangle_{ap}^j = |H\rangle_S^j |1_{M_L}\rangle^j + e^{i\varphi_S}|V\rangle_S^j |1_{M_R}\rangle^j \tag{1}$$

$|H\rangle_S^j$ ($|V\rangle_S^j$) denotes an H (V)-polarized Stokes photon, $|1_{M_L}\rangle^j$ ($|1_{M_R}\rangle^j$) denotes an SW excitation in M_R^j (M_L^j), and φ_S is the relative phase between the two Stokes emissions along the A_L and A_R arms created in any of the temporal modes. In this experiment, the excitation probabilities for the various temporal modes are basically symmetrical, i.e., $\chi_1 \approx \cdots \chi_j \cdots \approx \chi_m \approx \chi$. To retrieve the jth SW qubit, the jth read pulse with a wave-vector of $\mathbf{k}_r^j = -\mathbf{k}_w^j$ is applied to the atomic ensemble through $\mathrm{BS_2}$, thus converting the SW M_R^j (M_L^j) into an anti-Stokes photon AS_R^j (AS_L^j) with a wave-vector $\mathbf{k}_{AS_R} = \mathbf{k}_w^j - \mathbf{k}_{S_R} + \mathbf{k}_r^j = -\mathbf{k}_{S_R}$ ($\mathbf{k}_{AS_L} = \mathbf{k}_w^j - \mathbf{k}_{S_L} + \mathbf{k}_r^j = -\mathbf{k}_{S_L}$) [44]. The two anti-Stokes photons AS_R^j and AS_L^j with $j=1$ to m propagate in the A_R (A_L) arms in the direction opposite to that of S_R^j (S_L^j), where they are then combined after $\mathrm{BD_2}$. The two-photon entangled state is written as follows:

$$|\Phi\rangle_{pp}^j = |H\rangle_S^j |H\rangle_{AS}^j + e^{i(\varphi_S+\varphi_{AS})}|V\rangle_S^j |V\rangle_{AS}^j \tag{2}$$

where the subscript AS denotes anti-Stokes photons and φ_{AS} is the relative phase between the two anti-Stokes fields propagating in arms A_L and A_R. The sum of φ_S and φ_{AS} is set to zero using a phase compensator [91]. The anti-Stokes fields in arms A_L and A_R are transformed from the σ^+-polarization into H-polarized fields by the $\lambda/4$-wave-plate labeled as $\mathrm{QW_{AS}}$ in Fig. 1(a). Furthermore, the anti-Stokes field in arm A_R is transformed into a V-polarized field by the $\lambda/2$-wave-plate labeled as $\mathrm{HW_{AS}}$ in Fig. 1(a). Both fields are combined into an anti-Stokes qubit AS_{qbit}^j by $\mathrm{BD_2}$ and subsequently propagate in the A_{00} mode along the clockwise direction. As shown in Fig. 1(a), the escaped Stokes (anti-Stokes) photon from the OC is coupled to a single-mode fiber $\mathrm{SMF_S}$ ($\mathrm{SMF_{AS}}$) and is then guided into polarization-beam splitter $\mathrm{PBS_S}$ ($\mathrm{PBS_{AS}}$). The two outputs of $\mathrm{PBS_S}$ ($\mathrm{PBS_{AS}}$) are sent to the single-photon detectors $\mathrm{D_{S1}}$ ($\mathrm{D_{AS1}}$) and $\mathrm{D_{S2}}$ ($\mathrm{D_{AS2}}$) for polarization projection measurement (PPM). We placed optical-spectrum-filter sets (OSFSs) before the PPM to suppress noise from the write beams, the read beams, and leakage from the locking beam. The polarization angle θ_S (θ_{AS}) of the Stokes (anti-Stokes) field can be changed by rotating the wave-plate (WP) before $\mathrm{PBS_S}$ ($\mathrm{PBS_{AS}}$).

Optics EXPRESS

3. Experimental results

To characterize the temporally multiplexed entanglement interface, we first measured its retrieval efficiency. The intrinsic retrieval efficiency of the temporally multiplexed entanglement interface is defined as $\gamma^{(m)} = \sum_{j=1}^{m} P^j_{S,AS} / \left(\eta_{DAS} \sum_{j=1}^{m} P^j_S\right)$, where m is the number of multiplexed modes. $P^j_{S,AS} = P^j_{D_{S1},D_{AS1}} + P^j_{D_{S2},D_{AS2}} + P^j_{D_{S1},D_{AS2}} + P^j_{D_{S2},D_{AS1}}$ is the success probability of coincidence counting between the Stokes and anti-Stokes photons in the jth temporal mode (in detection window S_j), and $P^j_{D_{S1}(D_{S2}),D_{AS1}(D_{AS2})}$ is the coincidence probability between detectors D_{S1} (D_{S2}) and D_{AS1} (D_{AS2}) in the jth temporal mode. $P^j_S = P^j_{D_{S1}} + P^j_{D_{S2}}$ is the probability of detection of a Stokes photon in the jth temporal mode, and $P^j_{D_{S1}}(P^j_{D_{S2}})$ is the detection probability for the Stokes detector D_{S1} (D_{S2}). $\eta_{DAS} = \eta_e \times \eta_{AS}$ is the total detection efficiency for the anti-Stokes photon, where $\eta_e \approx 0.55$ denotes its escape efficiency from the cavity and $\eta_{AS} \approx 0.25$ denotes the detection efficiency of the anti-Stokes channel, which includes the coupling efficiency of SMF_{AS} ($\eta_{SMF} \approx 0.72$), the transmission of the OSFS ($\eta_{OSFS} \approx 0.56$), the transmission of the multi-mode fiber ($\eta_{MMF} \approx 0.91$), and the detection efficiency of D_{AS1} and D_{AS2} ($\eta_D \approx 0.68$). $P^j_{S,AS}$ and P^j_S are measured when the polarization angles for the Stokes and anti-Stokes photons are set to be $\theta_S = \theta_{AS} = 0°$.

Figure 2 shows the intrinsic retrieval efficiency $\gamma^{(m)}$ as a function of the storage time t. At the zero delay, where $t = 0$, the intrinsic retrieval efficiency is 70.4 ± 1.9%, which is only ~16% in our previous work [64,81]. We fit the measured retrieval efficiency using the function $\gamma^{(12)}(t) = \frac{\gamma_0}{2}(e^{-(t/t_0)^2} + e^{-t/t_0})$ with an initial retrieval efficiency of $\gamma_0 = 0.71$ and a 1/e storage lifetime of $t_0 = 262$ μs. Note that in all measurements, the excitation probability for each single-mode Stokes photon was adjusted to be $\chi \approx 1\%$ to avoid multiple excitations.

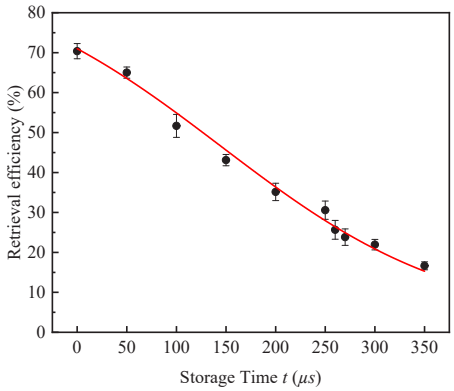

Fig. 2. Intrinsic retrieval efficiency of the 12-temporal-mode multiplexed entanglement source as a function of the storage time t. The red line is given by the fitting function $\gamma^{(12)}(t) = \frac{\gamma_0}{2}(e^{-(t/t_0)^2} + e^{-t/t_0})$ with $\gamma_0 = 0.71$ and $t_0 = 262$ μs.

Next, we verify the entanglement property of the multiplexed atom-photon interface by measuring the Clauser-Horne-Shimony-Holt (CHSH) inequality. The $S^{(m)}$ parameter for the multiplexed entanglement with m modes is defined as $S^{(m)} = |E^{(m)}(\theta_S, \theta_{AS}) - E^{(m)}(\theta_S, \theta'_{AS}) + E^{(m)}(\theta'_S, \theta_{AS}) + E^{(m)}(\theta'_S, \theta'_{AS})|$, where θ_S and θ'_S (θ_{AS} and θ'_{AS}) are the polarization angles for the Stokes (anti-Stokes) photon. The correlation function $E^{(m)}(\theta_S, \theta_{AS})$ is given by:

$$\frac{C^{(m)}_{D_{S1}D_{AS1}}(\theta_S, \theta_{AS}) + C^{(m)}_{D_{S2}D_{AS2}}(\theta_S, \theta_{AS}) - C^{(m)}_{D_{S1}D_{AS2}}(\theta_S, \theta_{AS}) - C^{(m)}_{D_{S2}D_{AS1}}(\theta_S, \theta_{AS})}{C^{(m)}_{D_{S1}D_{AS1}}(\theta_S, \theta_{AS}) + C^{(m)}_{D_{S2}D_{AS2}}(\theta_S, \theta_{AS}) + C^{(m)}_{D_{S1}D_{AS2}}(\theta_S, \theta_{AS}) + C^{(m)}_{D_{S2}D_{AS1}}(\theta_S, \theta_{AS})} \tag{3}$$

Optics EXPRESS

Here, $C^{(m)}_{D_{S1}D_{AS1}}(\theta_S, \theta_{AS})$, $C^{(m)}_{D_{S2}D_{AS2}}(\theta_S, \theta_{AS})$, $C^{(m)}_{D_{S1}D_{AS2}}(\theta_S, \theta_{AS})$, and $C^{(m)}_{D_{S2}D_{AS1}}(\theta_S, \theta_{AS})$ are the coincidence counts between detectors D_{S1}/D_{S2} and D_{AS1}/D_{AS2}. By setting $\theta_S = 0°$, $\theta'_S = 45°$, $\theta_{AS} = 22.5°$, and $\theta'_{AS} = 67.5°$, we measured the Bell parameter $S^{(12)}$ as a function of the storage time t, as indicated by the black squares in Fig. 3. At the beginning of the storage time ($t = 0$ μs), the measured S parameter is 2.21(2), which violates the CHSH inequality $S^{(12)} \leq 2$ by 10.5 standard deviations. At the later storage time $t = 125$ μs, the measured S parameter is 2.01(2), which still violates the CHSH inequality.

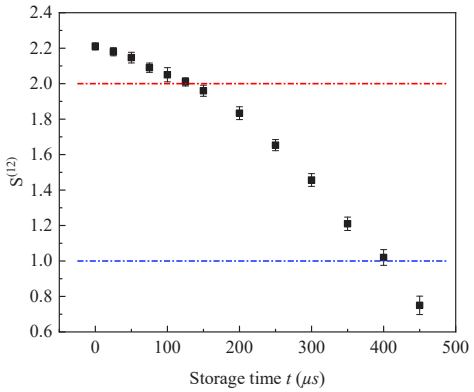

Fig. 3. Measured Bell parameter $S^{(12)}$ as a function of the storage time t. The error bars represent the standard deviations of the measured values.

Next, we study the generation probability of the temporally multiplexed photon-atom entanglement interface. Detection of the Stokes photon heralds generation of the photon-atom entanglement. The generation probability of the multiplexed photon-atom entanglement with m modes is proportional to the detection probability of the Stokes photon $P^{(m)}_S$, which is measured as the sum of the detection probabilities $P^{(m)}_{S_1}$ and $P^{(m)}_{S_2}$ by detectors D_{S1} and D_{S2}. Here, the polarization angle for the Stokes photon $\theta_S = 0°$. For $\chi \ll 1$, the detection probability of the Stokes photon for the multiplexed photon-atom entanglement can be expressed as $P^{(m)}_S = P^{(m)}_{S_1} + P^{(m)}_{S_2} = 1 - (1 - P^j_S)^m \approx mP^j_S$ [71,74], where P^j_S is the detection probability of the Stokes photon for a nonmultiplexed entanglement source. Figure 4 shows the measured $P^{(m)}_S$ as a function of m for $\chi \approx 1\%$. The results show that $P^{(m)}_S$ increases linearly with increasing m, and that $P^{(12)}_S/P^{(1)}_S \approx 12.1 \pm 0.2$, which is in general agreement with the expected results. This result implies that our multiplexed entanglement source achieves a 12-fold increase in the generation probability of the atom-photon entanglement.

To evaluate the generation probability of the polarization-entangled photon pair per trial, we measured the coincidence probability between the Stokes and anti-Stokes photons. The generation probability is measured as the coincidence count between the Stokes and anti-Stokes photons $P^{(m)}_{S,AS}$ at $\theta_S = \theta_{AS} = 0°$. The coincidence count probability can be expressed as $P^{(m)}_{S,AS} = \sum_{j=1}^{m}((P^j_{D_{S1}} + P^j_{D_{S2}})\gamma_j\eta_{DAS})$, where γ_j is the retrieval efficiency of the jth mode of the spin-wave excitation. Figure 5 shows the measured $P^{(m)}_{S,AS}$ as a function of mode number m. When $m = 12$, $P^{(12)}_{S,AS}/P^{(1)}_{S,AS} \approx 11.6$. We also measured the Bell parameters $S^{(m)}$ of the multiplexed entanglement source as a function of m. The measured $S^{(m)}$ was equal to 2.45(2) for $m = 1$ and decreased as m increased. This reduction is attributed to the additional noise from unwanted spin waves that are associated with undetected Stokes photons [73,81]. This issue can be overcome by using an asymmetric channel to collect the Stokes and anti-Stokes photons [64].

Optics EXPRESS

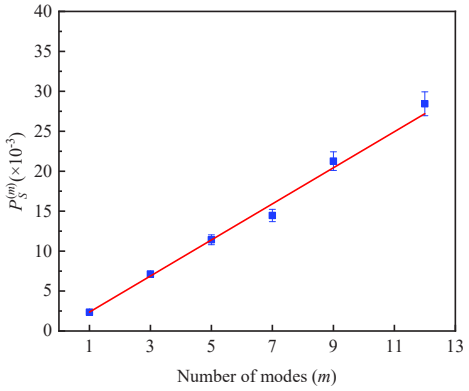

Fig. 4. Detection probability $P_S^{(m)}$ of the Stokes photon as a function of mode number m. The red line is a linear fitting of the measured data.

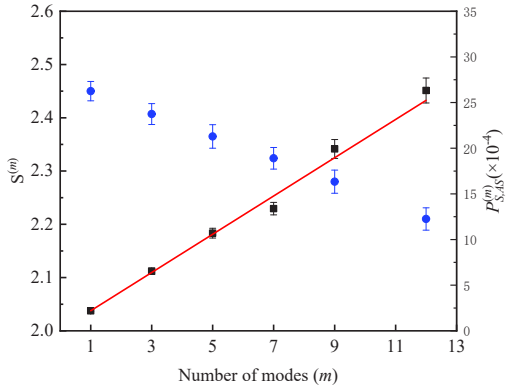

Fig. 5. Measured coincidence probability $P_{S,AS}^{(m)}$ (black squares) of the Stokes-anti-Stokes photons and the Bell parameter $S^{(m)}$ (blue dots) as a function of mode number m. The red line is a linear fitting of the measured $P_{S,AS}^{(m)}$.

4. Conclusion

We demonstrate a high-retrieval-efficiency and temporally-multiplexed atom-photon entanglement interface. This multiplexed interface generates atom-photon entanglement in up to 12 pairs of spin-wave and photon modes and then increases the probability of the entanglement generation by a factor of ~12, compared to the non-multiplexed interface. A ring cavity is used to enhance the retrieval fields from the spin-wave qubits, thus the intrinsic retrieval efficiency reaches $70.4 \pm 1.9\%$. The multiplexed atom-photon interface uses a feedforward-controlled readout system. The multiplexed spin waves are converted into anti-Stokes photons propagating in a well-defined spatio-temporal mode. The measured Bell parameter for the multiplexed atom-photon entanglement is 2.21(2), and is combined with a memory lifetime of up to ~125 μs. The additional noise generated during the multimode preparation process degrades the quality of the atom-photon entanglement interface, which may be suppressed by using an asymmetric channel to collect the Stokes and anti-Stokes photons [64] in the future. In our scheme, a magnetically-insensitive state is selected to store the quantum information; this approach has the potential to improve the lifetime of the memory qubit by more than three orders of magnitude if

Optics EXPRESS

atoms are being loaded into an optical lattice [52]. Next, we intend to consider combining m temporal modes and n spatial modes into one memory system, thus allowing an atom-photon entanglement source with high retrieval efficiency and large-scale ($m \times n$) multiplexing capability to be realized.

In summary, the presented work is the first experimental demonstration of an atom-photon entanglement source having a multiplexed storage capacity and high retrieval efficiency simultaneously, which represents an important step towards the development of a multiplexed QR [71,72].

Funding. Ministry of Science and Technology of the People's Republic of China (2016YFA0301402); National Natural Science Foundation of China (12174235, 11834010); Fund for Shanxi Key Subjects Construction (1331).

Disclosures. The authors declare no conflicts of interest.

Data availability. Data underlying the results presented in this paper are not publicly available at this time but may be obtained from the authors upon reasonable request.

References

1. L. M. Duan, M. D. Lukin, J. I. Cirac, and P. Zoller, "Long-distance quantum communication with atomic ensembles and linear optics," Nature **414**(6862), 413–418 (2001).
2. N. Sangouard, C. Simon, H. de Riedmatten, and N. Gisin, "Quantum repeaters based on atomic ensembles and linear optics," Rev. Mod. Phys. **83**(1), 33–80 (2011).
3. H. J. Kimble, "The quantum internet," Nature **453**(7198), 1023–1030 (2008).
4. H. J. Briegel, W. Dür, J. I. Cirac, and P. Zoller, "Quantum Repeaters: The Role of Imperfect Local Operations in Quantum Communication," Phys. Rev. Lett. **81**(26), 5932–5935 (1998).
5. B. Zhao, Z.-B. Chen, Y.-A. Chen, J. Schmiedmayer, and J.-W. Pan, "Robust Creation of Entanglement between Remote Memory Qubits," Phys. Rev. Lett. **98**(24), 240502 (2007).
6. Z.-S. Yuan, Y.-A. Chen, B. Zhao, S. Chen, J. Schmiedmayer, and J.-W. Pan, "Experimental demonstration of a BDCZ quantum repeater node," Nature **454**(7208), 1098–1101 (2008).
7. C. Liu, Z. Dutton, C. H. Behroozi, and L. V. Hau, "Observation of coherent optical information storage in an atomic medium using halted light pulses," Nature **409**(6819), 490–493 (2001).
8. D. F. Phillips, A. Fleischhauer, A. Mair, R. L. Walsworth, and M. D. Lukin, "Storage of Light in Atomic Vapor," Phys. Rev. Lett. **86**(5), 783–786 (2001).
9. M. D. Eisaman, A. André, F. Massou, M. Fleischhauer, A. S. Zibrov, and M. D. Lukin, "Electromagnetically induced transparency with tunable single-photon pulses," Nature **438**(7069), 837–841 (2005).
10. T. Chanelière, D. N. Matsukevich, S. D. Jenkins, S. Y. Lan, T. A. B. Kennedy, and A. Kuzmich, "Storage and retrieval of single photons transmitted between remote quantum memories," Nature **438**(7069), 833–836 (2005).
11. S. Zhou, S. Zhang, C. Liu, J. F. Chen, J. Wen, M. M. T. Loy, G. K. L. Wong, and S. Du, "Optimal storage and retrieval of single-photon waveforms," Opt. Express **20**(22), 24124–24131 (2012).
12. Z. Xu, Y. Wu, L. Tian, L. Chen, Z. Zhang, Z. Yan, S. Li, H. Wang, C. Xie, and K. Peng, "Long Lifetime and High-Fidelity Quantum Memory of Photonic Polarization Qubit by Lifting Zeeman Degeneracy," Phys. Rev. Lett. **111**(24), 240503 (2013).
13. G. Heinze, C. Hubrich, and T. Halfmann, "Stopped Light and Image Storage by Electromagnetically Induced Transparency up to the Regime of One Minute," Phys. Rev. Lett. **111**(3), 033601 (2013).
14. Y.-H. Chen, M.-J. Lee, I. C. Wang, S. Du, Y.-F. Chen, Y.-C. Chen, and I. A. Yu, "Coherent Optical Memory with High Storage Efficiency and Large Fractional Delay," Phys. Rev. Lett. **110**(8), 083601 (2013).
15. Z. Yan, L. Wu, X. Jia, Y. Liu, R. Deng, S. Li, H. Wang, C. Xie, and K. Peng, "Establishing and storing of deterministic quantum entanglement among three distant atomic ensembles," Nat. Commun. **8**(1), 718 (2017).
16. Y.-F. Hsiao, P.-J. Tsai, H.-S. Chen, S.-X. Lin, C.-C. Hung, C.-H. Lee, Y.-H. Chen, Y.-F. Chen, I. A. Yu, and Y.-C. Chen, "Highly Efficient Coherent Optical Memory Based on Electromagnetically Induced Transparency," Phys. Rev. Lett. **120**(18), 183602 (2018).
17. P. Vernaz-Gris, K. Huang, M. Cao, A. S. Sheremet, and J. Laurat, "Highly-efficient quantum memory for polarization qubits in a spatially-multiplexed cold atomic ensemble," Nat. Commun. **9**(1), 363 (2018).
18. Y. Wang, J. Li, S. Zhang, K. Su, Y. Zhou, K. Liao, S. Du, H. Yan, and S.-L. Zhu, "Efficient quantum memory for single-photon polarization qubits," Nat. Photonics **13**(5), 346–351 (2019).
19. L. Ma, X. Lei, J. Yan, R. Li, T. Chai, Z. Yan, X. Jia, C. Xie, and K. Peng, "High-performance cavity-enhanced quantum memory with warm atomic cell," Nat. Commun. **13**(1), 2368 (2022).
20. E. Saglamyurek, N. Sinclair, J. Jin, J. A. Slater, D. Oblak, F. Bussières, M. George, R. Ricken, W. Sohler, and W. Tittel, "Broadband waveguide quantum memory for entangled photons," Nature **469**(7331), 512–515 (2011).
21. Y. W. Cho, G. T. Campbell, J. L. Everett, J. Bernu, D. B. Higginbottom, M. T. Cao, J. Geng, N. P. Robins, P. K. Lam, and B. C. Buchler, "Highly efficient optical quantum memory with long coherence time in cold atoms," Optica **3**(1), 100–107 (2016).

Optics EXPRESS

22. C. Clausen, I. Usmani, F. Bussières, N. Sangouard, M. Afzelius, H. de Riedmatten, and N. Gisin, "Quantum storage of photonic entanglement in a crystal," Nature **469**(7331), 508–511 (2011).
23. M. Hosseini, G. Campbell, B. M. Sparkes, P. K. Lam, and B. C. Buchler, "Unconditional room-temperature quantum memory," Nat. Phys. **7**(10), 794–798 (2011).
24. M. Sabooni, Q. Li, S. Kröll, and L. Rippe, "Efficient Quantum Memory Using a Weakly Absorbing Sample," Phys. Rev. Lett. **110**(13), 133604 (2013).
25. N. Sinclair, E. Saglamyurek, H. Mallahzadeh, J. A. Slater, M. George, R. Ricken, M. P. Hedges, D. Oblak, C. Simon, W. Sohler, and W. Tittel, "Spectral Multiplexing for Scalable Quantum Photonics using an Atomic Frequency Comb Quantum Memory and Feed-Forward Control," Phys. Rev. Lett. **113**(5), 053603 (2014).
26. E. Saglamyurek, J. Jin, V. B. Verma, M. D. Shaw, F. Marsili, S. W. Nam, D. Oblak, and W. Tittel, "Quantum storage of entangled telecom-wavelength photons in an erbium-doped optical fibre," Nat. Photonics **9**(2), 83–87 (2015).
27. K. R. Ferguson, S. E. Beavan, J. J. Longdell, and M. J. Sellars, "Generation of Light with Multimode Time-Delayed Entanglement Using Storage in a Solid-State Spin-Wave Quantum Memory," Phys. Rev. Lett. **117**(2), 020501 (2016).
28. H. de Riedmatten, M. Afzelius, M. U. Staudt, C. Simon, and N. Gisin, "A solid-state light–matter interface at the single-photon level," Nature **456**(7223), 773–777 (2008).
29. M. Afzelius, C. Simon, H. de Riedmatten, and N. Gisin, "Multimode quantum memory based on atomic frequency combs," Phys. Rev. A **79**(5), 052329 (2009).
30. C. Simon, M. Afzelius, J. Appel, A. Boyer de la Giroday, S. J. Dewhurst, N. Gisin, C. Y. Hu, F. Jelezko, S. Kröll, J. H. Müller, J. Nunn, E. S. Polzik, J. G. Rarity, H. De Riedmatten, W. Rosenfeld, A. J. Shields, N. Sköld, R. M. Stevenson, R. Thew, I. A. Walmsley, M. C. Weber, H. Weinfurter, J. Wrachtrup, and R. J. Young, "Quantum memories," The European Physical Journal D **58**(1), 1–22 (2010).
31. E. Saglamyurek, M. Grimau Puigibert, Q. Zhou, L. Giner, F. Marsili, V. B. Verma, S. Woo Nam, L. Oesterling, D. Nippa, D. Oblak, and W. Tittel, "A multiplexed light-matter interface for fibre-based quantum networks," Nat. Commun. **7**(1), 11202 (2016).
32. C. Liu, T.-X. Zhu, M.-X. Su, Y.-Z. Ma, Z.-Q. Zhou, C.-F. Li, and G.-C. Guo, "On-Demand Quantum Storage of Photonic Qubits in an On-Chip Waveguide," Phys. Rev. Lett. **125**(26), 260504 (2020).
33. X. Liu, J. Hu, Z.-F. Li, X. Li, P.-Y. Li, P.-J. Liang, Z.-Q. Zhou, C.-F. Li, and G.-C. Guo, "Heralded entanglement distribution between two absorptive quantum memories," Nature **594**(7861), 41–45 (2021).
34. T.-X. Zhu, C. Liu, M. Jin, M.-X. Su, Y.-P. Liu, W.-J. Li, Y. Ye, Z.-Q. Zhou, C.-F. Li, and G.-C. Guo, "On-Demand Integrated Quantum Memory for Polarization Qubits," Phys. Rev. Lett. **128**(18), 180501 (2022).
35. K. F. Reim, J. Nunn, V. O. Lorenz, B. J. Sussman, K. C. Lee, N. K. Langford, D. Jaksch, and I. A. Walmsley, "Towards high-speed optical quantum memories," Nat. Photonics **4**(4), 218–221 (2010).
36. D.-S. Ding, W. Zhang, Z.-Y. Zhou, S. Shi, B.-S. Shi, and G.-C. Guo, "Raman quantum memory of photonic polarized entanglement," Nat. Photonics **9**(5), 332–338 (2015).
37. K. T. Kaczmarek, P. M. Ledingham, B. Brecht, S. E. Thomas, G. S. Thekkadath, O. Lazo-Arjona, J. H. D. Munns, E. Poem, A. Feizpour, D. J. Saunders, J. Nunn, and I. A. Walmsley, "High-speed noise-free optical quantum memory," Phys. Rev. A **97**(4), 042316 (2018).
38. R. Finkelstein, E. Poem, O. Michel, O. Lahad, and O. Firstenberg, "Fast, noise-free memory for photon synchronization at room temperature," Sci. Adv. **4**(1), eaap8598 (2018).
39. J. Guo, X. Feng, P. Yang, Z. Yu, L. Q. Chen, C.-H. Yuan, and W. Zhang, "High-performance Raman quantum memory with optimal control in room temperature atoms," Nat. Commun. **10**(1), 148 (2019).
40. A. Kuzmich, W. P. Bowen, A. D. Boozer, A. Boca, C. W. Chou, L. M. Duan, and H. J. Kimble, "Generation of nonclassical photon pairs for scalable quantum communication with atomic ensembles," Nature **423**(6941), 731–734 (2003).
41. D. Felinto, C. W. Chou, H. de Riedmatten, S. V. Polyakov, and H. J. Kimble, "Control of decoherence in the generation of photon pairs from atomic ensembles," Phys. Rev. A **72**(5), 053809 (2005).
42. J. Laurat, H. de Riedmatten, D. Felinto, C.-W. Chou, E. W. Schomburg, and H. J. Kimble, "Efficient retrieval of a single excitation stored in an atomic ensemble," Opt. Express **14**(15), 6912–6918 (2006).
43. J. Simon, H. Tanji, J. K. Thompson, and V. Vuletić, "Interfacing Collective Atomic Excitations and Single Photons," Phys. Rev. Lett. **98**(18), 183601 (2007).
44. R. Zhao, Y. O. Dudin, S. D. Jenkins, C. J. Campbell, D. N. Matsukevich, T. A. B. Kennedy, and A. Kuzmich, "Long-lived quantum memory," Nat. Phys. **5**(2), 100–104 (2009).
45. B. Zhao, Y.-A. Chen, X.-H. Bao, T. Strassel, C.-S. Chuu, X.-M. Jin, J. Schmiedmayer, Z.-S. Yuan, S. Chen, and J.-W. Pan, "A millisecond quantum memory for scalable quantum networks," Nat. Phys. **5**(2), 95–99 (2009).
46. H. Tanji, S. Ghosh, J. Simon, B. Bloom, and V. Vuletić, "Heralded Single-Magnon Quantum Memory for Photon Polarization States," Phys. Rev. Lett. **103**(4), 043601 (2009).
47. A. G. Radnaev, Y. O. Dudin, R. Zhao, H. H. Jen, S. D. Jenkins, A. Kuzmich, and T. A. B. Kennedy, "A quantum memory with telecom-wavelength conversion," Nat. Phys. **6**(11), 894–899 (2010).
48. Y. O. Dudin, A. G. Radnaev, R. Zhao, J. Z. Blumoff, T. A. B. Kennedy, and A. Kuzmich, "Entanglement of Light-Shift Compensated Atomic Spin Waves with Telecom Light," Phys. Rev. Lett. **105**(26), 260502 (2010).
49. X.-H. Bao, A. Reingruber, P. Dietrich, J. Rui, A. Dück, T. Strassel, L. Li, N.-L. Liu, B. Zhao, and J.-W. Pan, "Efficient and long-lived quantum memory with cold atoms inside a ring cavity," Nat. Phys. **8**(7), 517–521 (2012).

Optics EXPRESS

50. E. Bimbard, R. Boddeda, N. Vitrant, A. Grankin, V. Parigi, J. Stanojevic, A. Ourjoumtsev, and P. Grangier, "Homodyne Tomography of a Single Photon Retrieved on Demand from a Cavity-Enhanced Cold Atom Memory," Phys. Rev. Lett. **112**(3), 033601 (2014).
51. S.-J. Yang, X.-J. Wang, J. Li, J. Rui, X.-H. Bao, and J.-W. Pan, "Highly Retrievable Spin-Wave–Photon Entanglement Source," Phys. Rev. Lett. **114**(21), 210501 (2015).
52. S.-J. Yang, X.-J. Wang, X.-H. Bao, and J.-W. Pan, "An efficient quantum light–matter interface with sub-second lifetime," Nat. Photonics **10**(6), 381–384 (2016).
53. C. Laplane, P. Jobez, J. Etesse, N. Gisin, and M. Afzelius, "Multimode and Long-Lived Quantum Correlations Between Photons and Spins in a Crystal," Phys. Rev. Lett. **118**(21), 210501 (2017).
54. K. Kutluer, M. Mazzera, and H. de Riedmatten, "Solid-State Source of Nonclassical Photon Pairs with Embedded Multimode Quantum Memory," Phys. Rev. Lett. **118**(21), 210502 (2017).
55. Y. F. Pu, N. Jiang, W. Chang, H. X. Yang, C. Li, and L. M. Duan, "Experimental realization of a multiplexed quantum memory with 225 individually accessible memory cells," Nat. Commun. **8**(1), 15359 (2017).
56. R. Ikuta, T. Kobayashi, T. Kawakami, S. Miki, M. Yabuno, T. Yamashita, H. Terai, M. Koashi, T. Mukai, T. Yamamoto, and N. Imoto, "Polarization insensitive frequency conversion for an atom-photon entanglement distribution via a telecom network," Nat. Commun. **9**(1), 1997 (2018).
57. Y. Yu, F. Ma, X.-Y. Luo, B. Jing, P.-F. Sun, R.-Z. Fang, C.-W. Yang, H. Liu, M.-Y. Zheng, X.-P. Xie, W.-J. Zhang, L.-X. You, Z. Wang, T.-Y. Chen, Q. Zhang, X.-H. Bao, and J.-W. Pan, "Entanglement of two quantum memories via fibres over dozens of kilometres," Nature **578**(7794), 240–245 (2020).
58. H. Li, J.-P. Dou, X.-L. Pang, T.-H. Yang, C.-N. Zhang, Y. Chen, J.-M. Li, I. A. Walmsley, and X.-M. Jin, "Heralding quantum entanglement between two room-temperature atomic ensembles," Optica **8**(6), 925–929 (2021).
59. K. B. Dideriksen, R. Schmieg, M. Zugenmaier, and E. S. Polzik, "Room-temperature single-photon source with near-millisecond built-in memory," Nat. Commun. **12**(1), 3699 (2021).
60. X.-J. Wang, S.-J. Yang, P.-F. Sun, B. Jing, J. Li, M.-T. Zhou, X.-H. Bao, and J.-W. Pan, "Cavity-Enhanced Atom-Photon Entanglement with Subsecond Lifetime," Phys. Rev. Lett. **126**(9), 090501 (2021).
61. S.-Z. Wang, M.-J. Wang, Y.-F. Wen, Z.-X. Xu, T.-F. Ma, S.-J. Li, and H. Wang, "Long-lived and multiplexed atom-photon entanglement interface with feed-forward-controlled readouts," Commun. Phys. **4**(1), 168 (2021).
62. Y.-F. Pu, S. Zhang, Y.-K. Wu, N. Jiang, W. Chang, C. Li, and L.-M. Duan, "Experimental demonstration of memory-enhanced scaling for entanglement connection of quantum repeater segments," Nat. Photonics **15**(5), 374–378 (2021).
63. Y. Li, Y. Wen, S. Wang, C. Liu, H. Liu, M. Wang, C. Sun, Y. Gao, S. Li, and H. Wang, "Generation of entanglement between a highly wave-packet-tunable photon and a spin-wave memory in cold atoms," Opt. Express **30**(2), 2792–2802 (2022).
64. Y. Li, Y.-F. Wen, M.-J. Wang, C. Liu, H.-L. Liu, S.-J. Li, Z.-X. Xu, and H. Wang, "Noise suppression in a temporal-multimode quantum memory entangled with a photon via an asymmetrical photon-collection channel," Phys. Rev. A **106**(2), 022610 (2022).
65. M. Afzelius, N. Gisin, and H. de Riedmatten, "Quantum memory for photons," Phys. Today **68**(12), 42–47 (2015).
66. K. Heshami, D. G. England, P. C. Humphreys, P. J. Bustard, V. M. Acosta, J. Nunn, and B. J. Sussman, "Quantum memories: emerging applications and recent advances," J. Mod. Opt. **63**(20), 2005–2028 (2016).
67. C. Simon, "Towards a global quantum network," Nat. Photonics **11**(11), 678–680 (2017).
68. F. Bussières, N. Sangouard, M. Afzelius, H. de Riedmatten, C. Simon, and W. Tittel, "Prospective applications of optical quantum memories," J. Mod. Opt. **60**(18), 1519–1537 (2013).
69. P. Jobez, I. Usmani, N. Timoney, C. Laplane, N. Gisin, and M. Afzelius, "Cavity-enhanced storage in an optical spin-wave memory," New J. Phys. **16**(8), 083005 (2014).
70. Y. Wen, P. Zhou, Z. Xu, L. Yuan, M. Wang, S. Wang, L. Chen, and H. Wang, "Cavity-enhanced and long-lived optical memories for two orthogonal polarizations in cold atoms," Opt. Express **28**(1), 360–368 (2020).
71. C. Simon, H. de Riedmatten, M. Afzelius, N. Sangouard, H. Zbinden, and N. Gisin, "Quantum Repeaters with Photon Pair Sources and Multimode Memories," Phys. Rev. Lett. **98**(19), 190503 (2007).
72. O. A. Collins, S. D. Jenkins, A. Kuzmich, and T. A. B. Kennedy, "Multiplexed Memory-Insensitive Quantum Repeaters," Phys. Rev. Lett. **98**(6), 060502 (2007).
73. C. Simon, H. de Riedmatten, and M. Afzelius, "Temporally multiplexed quantum repeaters with atomic gases," Phys. Rev. A **82**(1), 010304 (2010).
74. L. Tian, Z. Xu, L. Chen, W. Ge, H. Yuan, Y. Wen, S. Wang, S. Li, and H. Wang, "Spatial Multiplexing of Atom-Photon Entanglement Sources using Feedforward Control and Switching Networks," Phys. Rev. Lett. **119**(13), 130505 (2017).
75. I. Usmani, M. Afzelius, H. de Riedmatten, and N. Gisin, "Mapping multiple photonic qubits into and out of one solid-state atomic ensemble," Nat. Commun. **1**(1), 12 (2010).
76. M. Bonarota, J. L. Le Gouët, and T. Chanelière, "Highly multimode storage in a crystal," New J. Phys. **13**(1), 013013 (2011).
77. M. Hosseini, B. M. Sparkes, G. Hétet, J. J. Longdell, P. K. Lam, and B. C. Buchler, "Coherent optical pulse sequencer for quantum applications," Nature **461**(7261), 241–245 (2009).
78. M. Hosseini, B. M. Sparkes, G. Campbell, P. K. Lam, and B. C. Buchler, "High efficiency coherent optical memory with warm rubidium vapour," Nat. Commun. **2**(1), 174 (2011).

Optics EXPRESS

79. C. Laplane, P. Jobez, J. Etesse, N. Timoney, N. Gisin, and M. Afzelius, "Multiplexed on-demand storage of polarization qubits in a crystal," New J. Phys. **18**(1), 013006 (2015).
80. J.-S. Tang, Z.-Q. Zhou, Y.-T. Wang, Y.-L. Li, X. Liu, Y.-L. Hua, Y. Zou, S. Wang, D.-Y. He, G. Chen, Y.-N. Sun, Y. Yu, M.-F. Li, G.-W. Zha, H.-Q. Ni, Z.-C. Niu, C.-F. Li, and G.-C. Guo, "Storage of multiple single-photon pulses emitted from a quantum dot in a solid-state quantum memory," Nat. Commun. **6**(1), 8652 (2015).
81. Y. Wen, P. Zhou, Z. Xu, L. Yuan, H. Zhang, S. Wang, L. Tian, S. Li, and H. Wang, "Multiplexed spin-wave–photon entanglement source using temporal multimode memories and feedforward-controlled readout," Phys. Rev. A **100**(1), 012342 (2019).
82. P. Caspar, E. Verbanis, E. Oudot, N. Maring, F. Samara, M. Caloz, M. Perrenoud, P. Sekatski, A. Martin, N. Sangouard, H. Zbinden, and R. T. Thew, "Heralded Distribution of Single-Photon Path Entanglement," Phys. Rev. Lett. **125**(11), 110506 (2020).
83. N. Jiang, Y. F. Pu, W. Chang, C. Li, S. Zhang, and L. M. Duan, "Experimental realization of 105-qubit random access quantum memory," npj Quantum Inf. **5**(1), 28 (2019).
84. Y. Pu, Y. Wu, N. Jiang, W. Chang, C. Li, S. Zhang, and L. Duan, "Experimental entanglement of 25 individually accessible atomic quantum interfaces," Sci. Adv. **4**(4), eaar3931 (2018).
85. M. Gündoğan, M. Mazzera, P. M. Ledingham, M. Cristiani, and H. de Riedmatten, "Coherent storage of temporally multimode light using a spin-wave atomic frequency comb memory," New J. Phys. **15**(4), 045012 (2013).
86. M. Lipka, M. Mazelanik, A. Leszczyński, W. Wasilewski, and M. Parniak, "Massively-multiplexed generation of Bell-type entanglement using a quantum memory," Commun. Phys. **4**(1), 46 (2021).
87. A. Seri, D. Lago-Rivera, A. Lenhard, G. Corrielli, R. Osellame, M. Mazzera, and H. de Riedmatten, "Quantum Storage of Frequency-Multiplexed Heralded Single Photons," Phys. Rev. Lett. **123**(8), 080502 (2019).
88. B. Albrecht, P. Farrera, G. Heinze, M. Cristiani, and H. de Riedmatten, "Controlled Rephasing of Single Collective Spin Excitations in a Cold Atomic Quantum Memory," Phys. Rev. Lett. **115**(16), 160501 (2015).
89. L. Heller, P. Farrera, G. Heinze, and H. de Riedmatten, "Cold-Atom Temporally Multiplexed Quantum Memory with Cavity-Enhanced Noise Suppression," Phys. Rev. Lett. **124**(21), 210504 (2020).
90. K. C. Cox, D. H. Meyer, Z. A. Castillo, F. K. Fatemi, and P. D. Kunz, "Spin-Wave Multiplexed Atom-Cavity Electrodynamics," Phys. Rev. Lett. **123**(26), 263601 (2019).
91. M. Wang, S. Wang, T. Ma, Y. Li, Y. Xie, H. Jiao, H. Liu, S. Li, and H. Wang, "Generation of highly retrievable atom photon entanglement with a millisecond lifetime via a spatially multiplexed cavity," arXiv, arXiv:2204.05794 [quant-ph] (2023).
92. M. Parniak, M. Dąbrowski, M. Mazelanik, A. Leszczyński, M. Lipka, and W. Wasilewski, "Wavevector multiplexed atomic quantum memory via spatially-resolved single-photon detection," Nat. Commun. **8**(1), 2140 (2017).